THE JOURNAL OF PHYSICAL CHEMISTRY B

Article

pubs.acs.org/JPCB

Temperature Determination by EPR at 275 GHz and the Detection of Temperature Jumps in Aqueous Samples

Mykhailo Azarkh and Edgar J. J. Groenen*

Huygens-Kamerlingh Onnes Laboratory, Department of Physics, Leiden University, P.O. Box 9504, 2300 RA Leiden, The Netherlands

Supporting Information

ABSTRACT: Second-moment analysis along two dimensions of continuous-wave EPR spectra of nitroxides enables EPR thermometry in a broad temperature range. Simulations show that the temperature can be derived in both the slow-motion and the fast-motion regime, which is experimentally verified at 275 GHz for H_2O/glycerol (50/50% by volume) and pure water. We demonstrate that this tool allows the calibration of temperature jumps induced by infrared laser irradiation of a submicroliter sample in the single-mode cavity of a 275 GHz spectrometer, which prepares for kinetic studies of processes involving paramagnetic species.

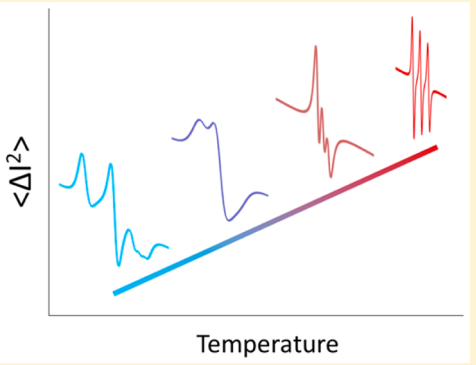

INTRODUCTION

Reorientational motion determines the shape of EPR spectra of nitroxides in the condensed phase. In the frozen state, the so-called rigid limit, the EPR spectrum of nitroxides is broad, and its width is set by the anisotropy of the electron−Zeeman and hyperfine interactions.[1] This anisotropy is less manifest when the nitroxide undergoes rotation in solution. In the slow-motion regime of rotation, the width of the spectrum decreases and the line shape changes in a complex way.[2] In the fast-motion regime, the Redfield limit, the width of the spectrum is determined by isotropic magnetic interactions, and the line width changes according to the motional narrowing theory.[3] Which motional regime applies to a particular EPR spectrum depends on the microwave frequency ω_{mw}. In terms of the rotational correlation time τ_c, slow motion corresponds to $\tau_c > 1/\omega_{mw}$ and fast motion to $\tau_c < 1/\omega_{mw}$.[2−4]

The rotational correlation time depends on temperature, which implies that temperature measurements by EPR are feasible. Indeed, EPR-based thermometry has been demonstrated in solution, where the changes in the EPR spectra induced by the nitroxide rotation are calibrated against temperature.[5−7] The spectral changes are assessed by single-value parameters such as the spectral line width, the ratio of the intensities of the nitrogen hyperfine lines, the hyperfine splitting, or the rotational correlation time as obtained from spectral simulations. At the conventional microwave frequency of 9.5 GHz and ambient temperature, the reorientational motion of nitroxides in solution is in the regime of fast rotation. Thermometry based on EPR reaches the highest resolution in the slow-motion regime. For this reason the motion of nitroxides has been slowed down by conjugation of nitroxides to polypeptides[5] or incorporation inside a proteinaceous microsphere.[7] Alternatively, the applied microwave frequency has been increased, which means that the reorientation motion becomes slower on the EPR time scale.[8,9] For example, the rotation with τ_c on the order of nanoseconds is slow at 9.5 GHz, while the rotation with τ_c on the order of tens of picoseconds is still slow at 275 GHz. Consequently, the range of temperatures accessible by EPR at the highest resolution can be adjusted by selection of the proper microwave frequency.

We have investigated the possibilities to determine the temperature of a submicroliter sample in an EPR cavity at 275 GHz in order to prepare for temperature-jump experiments at this microwave frequency. Application of a temperature jump, a fast increase of the temperature of a sample, is a common approach to study the kinetics of (bio)chemical processes.[10−13] The first temperature-jump experiments were realized by the electrical discharge of a capacitor through a conducting solution.[14] With the introduction of pulse lasers, laser-induced temperature jumps became widely used for both indirect and direct heating of the solution.[15,16] Indirect heating utilizes dyes, which transform the absorbed photon into heat. For direct heating of aqueous solutions, infrared (IR) lasers are used to excite the first overtone of the OH-stretching vibration. The laser-induced temperature jump can be combined with many spectroscopic techniques to follow, for example, the kinetics of protein folding and of enzymatic reactions. The effects induced by the temperature jump are probed with isotopically edited infrared,[17−19] resonance Raman,[20] UV absorption,[21] fluorescence,[22,23] Förster resonance energy transfer (FRET),[24] circular

Received: August 27, 2015
Revised: September 30, 2015
Published: October 5, 2015

DOI: 10.1021/acs.jpcb.5b08353
J. Phys. Chem. B 2015, 119, 13416−13421

dichroism (CD),[25] or time-resolved optical rotatory dispersion (TRORD).[26] Combination of the temperature-jump trigger with electron paramagnetic resonance (EPR) spectroscopy will allow the study of (bio)molecular processes involving paramagnetic species.

Here, we report on the determination of the temperature of a nitroxide sample from the EPR spectrum at 275 GHz and on the calibration of temperature jumps. As a temperature-sensitive parameter, we introduce a second moment $\langle \Delta I^2 \rangle$, which presents a measure of the motional narrowing of the EPR spectrum. We show that in combination with the common second moment $\langle \Delta B_0^2 \rangle$, which measures the overall width of an EPR spectrum, temperature determination of a sample in the cavity of a 275 GHz spectrometer is feasible in a broad temperature range. We demonstrate that using this tool the magnitude of a laser-induced temperature jump can be measured in a temperature regime that is relevant for the study of reaction kinetics in aqueous solutions.

EXPERIMENTAL SECTION

For all measurements, a 2 mM solution of 2,2,6,6-tetramethylpiperidine-*N*-oxyl (TEMPONE, Sigma-Aldrich) in water/glycerol (50/50% by volume) or in pure water was used. The 275 GHz spectra were recorded on a home-built spectrometer equipped with a single-mode cavity having slits for optical irradiation.[27] Temperature control was realized in a He-flow cryostat CF935 equipped with an Intelligent Temperature Controller ITC (both from Oxford Instruments). The EPR spectra were measured with a microwave frequency of 275.7 GHz, microwave power of 0.015 μW, and magnetic field modulation at a frequency of 1.2 kHz. Further experimental parameters for H_2O were magnetic field range from 9816.2 to 9828.7 mT, modulation amplitude of 0.1 mT, sweep rate of 0.05 mT/s, and 512 experimental points. Further experimental parameters for H_2O/glycerol were magnetic field range from 9800 to 9850 mT, modulation amplitude of 0.2 mT, sweep rate of 0.1 mT/s, and 1024 experimental points. Subsequently, the experimental spectra in H_2O/glycerol were interpolated to 2048 experimental points.

Temperature jumps were generated by irradiation of water with IR light at 1550 nm. The source of irradiation was a laser diode HHF-110 (SemiNex) coupled to a fiber (105 μm core diameter). The fiber laser can be operated in the continuous-wave mode at the maximum optical power of 3.7 W. In the current setup, the optical power that reaches the sample is less than the power of the laser. The laser light is partially blocked by the slits of the cavity and reflected from the sample capillary. For sample irradiation, the laser was connected to a multimode fiber AFS105/125Y (Thorlabs), which had one flat-cleave end. This end of the fiber was fixed in front of the slits of the cavity at a distance of 3 mm. For temperature jumps, the starting point was determined by the temperature of the cryostat, which was kept constant. The laser was switched on, and the EPR spectra were recorded under continuous irradiation.

The EPR spectra of TEMPONE at 275 GHz for different rotational correlation times have been calculated with the EasySpin toolbox for Matlab by solving the stochastic Liouville equation.[2,28] The following interaction tensors were used in the simulations: **g** = [2.0083 2.0058 2.0030] and **A** = [18 18 99] MHz for the nitrogen hyperfine tensor. The **g**-tensor was determined from the frozen-solution spectrum at 275 GHz, and the **A**-tensor was taken from ref 29. The isotropic line width was taken 0.3 mT, and the number of points was set at 2048. The rotational correlation times for different temperatures were calculated from the corresponding viscosities of the H_2O/glycerol mixtures[30] and the hydrodynamic radius of the nitroxide. The latter was obtained from the simulation of the 275 GHz experimental spectrum of TEMPONE in water at 20 °C.

Before processing, the experimental spectra were corrected for an admixture of dispersion by taking a linear combination of the measured signal and its quadrature signal such that the negative and positive areas in the first-derivative spectrum were equal. The quadrature signal was generated from the Hilbert transformation of the measured absorption signal. The phase correction did not exceed 13° for any of the spectra. All experimental spectra were normalized to the area under the absorption curve.

RESULTS

Second-Moment Analysis of EPR Spectra of Nitroxides at 275 GHz. The second moment of a normalized distribution $f(x)$ is defined by $\langle \Delta x^2 \rangle = \int_{-\infty}^{+\infty} (x - \langle x \rangle)^2 f(x)\, dx$. It is a measure of the width of the distribution $f(x)$. Accordingly, the second moment $\langle \Delta B_0^2 \rangle$ presents a common way to characterize the width of an EPR spectrum. For example, the second moment $\langle \Delta B_0^2 \rangle$ of the spectrum in Figure 1a, the simulated and normalized absorption spectrum of a fast rotating nitroxide at 275 GHz, provides a measure of the overall width of the spectrum. For this second moment, the spectrum is considered as a probability distribution of resonance fields. An alternative way is to look at the spectrum as a probability distribution of intensities and to define $N(I)$ as the number of resonance fields corresponding to intensity I. In other words, the function $N(I)$ counts at each intensity the number of intersections of the EPR absorption spectrum with a horizontal line at this intensity. Figure 1b represents the distribution $N(I)$ corresponding to the spectrum in Figure 1a. We consider the second moment of the distribution $N(I)$, after normalization, as a second measure of the shape of the EPR spectrum. It will be indicated by $\langle \Delta I^2 \rangle$.

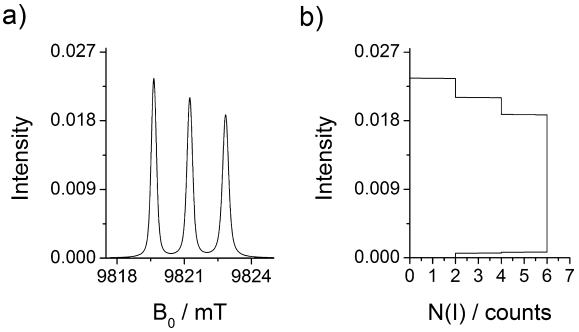

Figure 1. (a) Simulated normalized absorption spectrum of a nitroxide at 275 GHz. (b) The corresponding distribution of intensities.

Figure 2 illustrates distributions $N(I)$ corresponding to simulated EPR spectra of a nitroxide at 275 GHz. Figure 2a shows normalized spectra at four rotational correlation times, which vary from broad and unstructured to narrow three-line spectra with decreasing rotational correlation time. Figure 2b shows the corresponding normalized distributions $N(I)$, which become broader the smaller the rotational correlation time. Figure 3 combines the variation of the second moment $\langle \Delta I^2 \rangle$ of such distributions as a function of τ_c with the variation of the

DOI: 10.1021/acs.jpcb.5b08353
J. Phys. Chem. B 2015, 119, 13416−13421

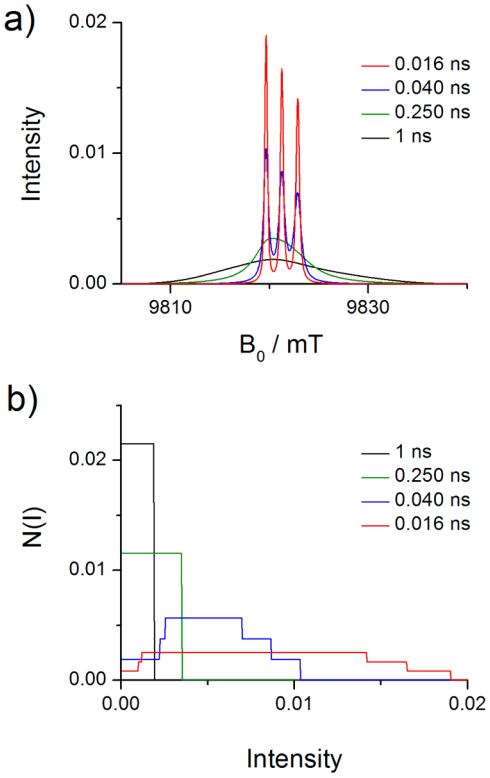

Figure 2. (a) Simulated normalized absorption spectra at 275 GHz of a nitroxide for different rotational correlation times. (b) Corresponding normalized distributions $N(I)$. The rotational correlation times are given in the figures.

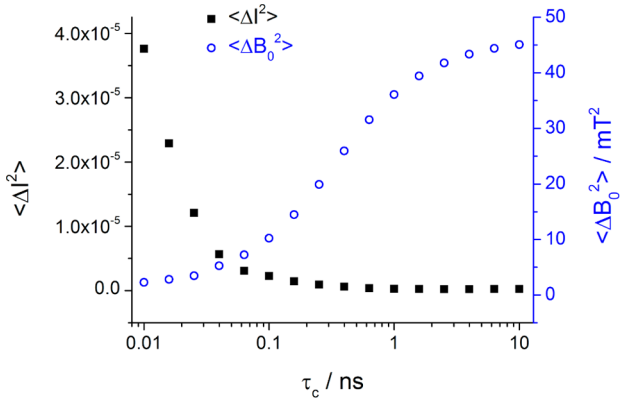

Figure 3. Second moments corresponding to the simulated spectra of a nitroxide at 275 GHz as a function of the rotational correlation time: (○) the second moment $\langle \Delta B_0^2 \rangle$ of the normalized absorption spectrum and (■) the second moment $\langle \Delta I^2 \rangle$ of the normalized distribution $N(I)$.

second moment $\langle \Delta B_0^2 \rangle$ for correlation times in the range of 10 ps to 10 ns.

At 275 GHz, the $\langle \Delta B_0^2 \rangle$ value is most sensitive to rotational motion for τ_c between 0.1 and 2 ns. For τ_c < 0.03 ns, the changes in the nitroxide spectrum are due to motional narrowing of the hyperfine lines. The width of the spectrum varies little, while the intensity changes significantly (cf. Figure 2a). These changes manifest themselves in $\langle \Delta I^2 \rangle$. As Figure 3 shows, the $\langle \Delta I^2 \rangle$ value is particularly sensitive to spectral changes for τ_c < 0.03 ns, which is the Redfield limit at 275 GHz.

Second Moments as a Measure of Temperature. The variation of $\langle \Delta I^2 \rangle$ and $\langle \Delta B_0^2 \rangle$ with τ_c suggests the use of these second moments as sensitive measures of temperature in a wide range of temperatures. In order to investigate this possibility, a series of 275 GHz EPR spectra were simulated for nitroxide in H_2O/glycerol mixtures. For all simulations, the isotropic line width and the hydrodynamic radius were kept constant (see Experimental Section), while the rotational correlation time was determined from the temperature and the viscosity of the solution. The variation of $\langle \Delta I^2 \rangle$ and $\langle \Delta B_0^2 \rangle$ with temperature was calculated for solutions with largely different viscosities. The simulations indicate that for solutions that contain more than 35% glycerol the $\langle \Delta B_0^2 \rangle$ value is a sensitive measure of temperature in the whole range from −30 to +30 °C (Figure S1a). The sensitivity of $\langle \Delta B_0^2 \rangle$ for temperatures above 0 °C decreases as the content of glycerol in the mixture decreases. The opposite trend is obtained for $\langle \Delta I^2 \rangle$, which is a sensitive measure of temperature above 0 °C. The value of $\langle \Delta I^2 \rangle$ increases more with increasing temperature for lower glycerol content and reaches the highest sensitivity for pure water (Figure S1b).

Experimental Determination of the Relation between Temperature and Second Moments. The predictions of the previous paragraph have been tested for TEMPONE in H_2O/glycerol (50/50% by volume). The EPR spectra at 275 GHz were measured in the temperature range from −30 to +30 °C, where the rotational motion of the nitroxide changes from the slow- to fast-motion regime (Figure S2). The value of $\langle \Delta B_0^2 \rangle$ decreases continuously with increasing temperature in this range while $\langle \Delta I^2 \rangle$ increases (Figure 4a). Both second moments can be used as a measure of temperature for this H_2O/glycerol mixture. This no longer applies to pure water, which has a much lower viscosity. The EPR spectra at 275 GHz were measured in the temperature range from 0 to +30 °C, where the nitroxide is in fast rotational motion (Figure S3). As shown in Figure 4b, the value of $\langle \Delta I^2 \rangle$ still increases strongly between 0 and +30 °C, but $\langle \Delta B_0^2 \rangle$ is virtually constant. The second moment $\langle \Delta I^2 \rangle$ remains a sensitive measure of temperature in this temperature range.

The sensitivity of the determination of temperature from $\langle \Delta I^2 \rangle$ values depends on the curvature of the calibration line in a particular temperature range. For example, for H_2O/glycerol between 20 and 25 °C, the variation of $\langle \Delta I^2 \rangle$ amounts to 0.06 × 10^{-6} per 1 °C. Differences of 0.02 × 10^{-6} in the value of $\langle \Delta I^2 \rangle$ can be reliably distinguished. The accuracy of temperature determination depends on the quality of the EPR spectra, e.g. baseline, signal-to-noise ratio. Repeated measurements in this temperature range on the same H_2O/glycerol sample at the same temperature setting of the cryostat resulted in $\langle \Delta I^2 \rangle$ values corresponding to the set temperature within 0.3 °C.

Temperature Jumps. The observed variation of $\langle \Delta I^2 \rangle$ with temperature in H_2O/glycerol and in H_2O has been used to calibrate laser-induced temperature jumps. Spectra of TEMPONE in H_2O/glycerol (50/50% by volume) have been recorded before and during irradiation with an IR laser at 1550 nm at various laser powers. For example, with the sample in the cryostat at −30 °C and irradiated by a laser power of 1.5 W the nitroxide spectra taken before and during irradiation correspond to $\langle \Delta I^2 \rangle$ values of 0.32 × 10^{-7} and 2.15 × 10^{-7}. Interpolation based on the calibration curve in Figure 4a shows that the temperature of the sample becomes −6 °C under this irradiation. A temperature jump of 24 °C is induced. An increase in the optical power to 3.5 W results in a temperature

DOI: 10.1021/acs.jpcb.5b08353
J. Phys. Chem. B 2015, 119, 13416−13421

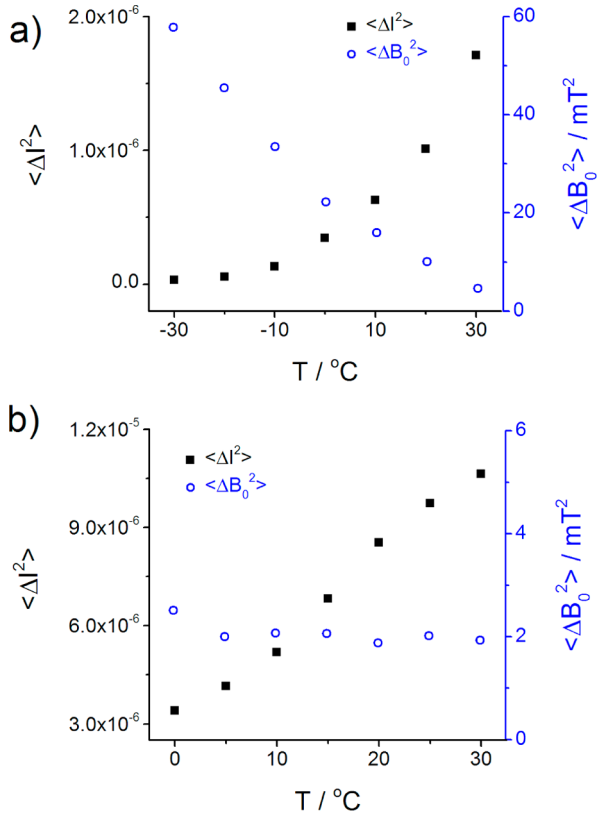

Figure 4. Second moments $\langle \Delta I^2 \rangle$ and $\langle \Delta B_0^2 \rangle$ corresponding to the experimental normalized EPR spectra of TEMPONE at 275 GHz as a function of temperature: (a) in H_2O/glycerol (50/50% by volume) and (b) in H_2O.

of the sample of 23 °C, which corresponds to a temperature jump of 53 °C. Similar experiments were performed for laser powers between 0.5 and 3.5 W at cryostat temperatures of −20 and −30 °C (Figure S4).

Temperature jumps in water, starting at temperatures below 0 °C, bring the sample from the frozen state, i.e., ice, to the liquid state. For example, starting at −20 °C, a temperature jump of 33 °C has been realized upon irradiation by the IR laser at an optical power of 2.5 W. Figure 5 summarizes the temperature jumps induced in H_2O/glycerol and H_2O (see also Figure S5).

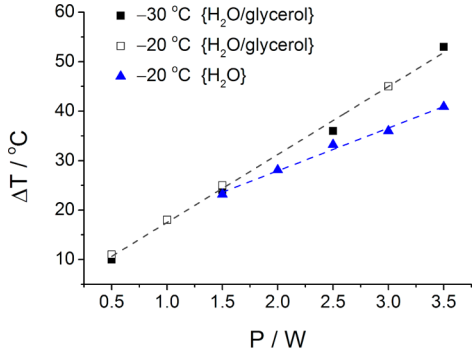

Figure 5. Laser-induced temperature jumps in H_2O/glycerol (50/50% by volume) and in H_2O as a function of optical power. Linear fits are shown with dashed lines. Starting temperatures before laser irradiation are given in the figure.

As a verification that the $\langle \Delta I^2 \rangle$ value provides a proper measure of the temperature jump, consider the 275 GHz EPR spectrum of TEMPONE in H_2O at a cryostat temperature of −20 °C upon 3.5 W laser irradiation. This spectrum corresponds to a $\langle \Delta I^2 \rangle$ value of 8.45×10^{-6}, which points to a temperature of the sample of about 20 °C (Figure 4b). Comparison of the spectrum with that obtained at a cryostat temperature of 20 °C shows that the two spectra are indeed virtually identical. Their superposition is represented in Figure S6.

DISCUSSION

Temperature measurements by EPR rely on the spectral response to the rotational motion of the nitroxide. The changes in the EPR spectrum at 275 GHz, as a consequence of the changes in this motion, have been assessed by two second-moment parameters, $\langle \Delta B_0^2 \rangle$ and $\langle \Delta I^2 \rangle$. While the first is more sensitive in the slow rotational regime, the second is more sensitive in the fast rotational regime. Together these parameters present a sensitive measure of temperature in a broad range of temperatures. The newly defined parameter $\langle \Delta I^2 \rangle$ has been used to quantify temperature jumps induced by IR laser irradiation, both in H_2O/glycerol and in H_2O.

Temperature measurements by EPR have been reported at X-band frequencies and utilize a line width or a ratio of intensities in the slow-motion spectra of nitroxides.[5,7] The changes in these parameters can be followed within a certain window of rotational motion where spectral lines do not merge or disappear. This window of rotational motion corresponds to a relatively narrow temperature range of approximately 15 °C.

The $\langle \Delta B_0^2 \rangle$ value, in contrast to the line width or the ratio of intensities, addresses the overall width of the spectrum, which changes over the entire slow-motion regime.[31,32] We demonstrate that at 275 GHz the second moment $\langle \Delta B_0^2 \rangle$ of slow-motion spectra of nitroxides is sensitive to temperature variations in a wide range, e.g., from −30 to +30 °C in H_2O/glycerol (50/50% by volume) (Figure 4a). In the limit of fast rotation, the overall width becomes virtually constant because the g and hyperfine anisotropies are averaged out. The second moment $\langle \Delta B_0^2 \rangle$ is no longer a sensitive measure of temperature, e.g., between 0 and 30 °C in water (Figure 4b). Increase in temperature for fast rotating nitroxides results in motional narrowing of the spectrum corresponding to an increase of the intensity (Figure 2). The second-moment parameter $\langle \Delta I^2 \rangle$ is found to be sensitive to these spectral changes (Figure 4b). The $\langle \Delta I^2 \rangle$ parameter extends the possibility to measure temperature by EPR to the fast-motion regime. The parameters $\langle \Delta B_0^2 \rangle$ and $\langle \Delta I^2 \rangle$ are complementary and together cover a broad range of temperatures. Which range depends on sample viscosity and microwave frequency. At 275 GHz, our experiments reveal that for H_2O/glycerol (50/50% by volume) temperatures between −30 and +30 °C are accessible. Previously, experiments were reported at X-band where the rotation of nitroxides was slowed down by conjugation of the nitroxide to polypeptides or by incorporation of the nitroxides into microspheres. The sensitivity of $\langle \Delta I^2 \rangle$ to temperature in the fast-motion regime eliminates the necessity to slow down nitroxide rotation.

In the motional-narrowing regime, the rotational correlation time provides an alternative to the second moments as a measure of temperature. Indeed, simulation of the experimental EPR spectra at 275 GHz of TEMPONE in H_2O/glycerol and in H_2O above 0 °C (Figures S2 and S3) shows the strong

DOI: 10.1021/acs.jpcb.5b08353
J. Phys. Chem. B 2015, 119, 13416−13421

dependence of the rotational correlation time on temperature (Figure S7). However, the second moments are useful in a broader temperature range and have the advantage that they are directly calculated from the experimental spectra with great accuracy.

We have used the second-moment parameter $\langle \Delta I^2 \rangle$ to examine the magnitude of temperature jumps that can be realized for submicroliter aqueous samples in the cylindrical microwave cavity of a 275 GHz EPR spectrometer. Laser-induced temperature jumps of a sample in such a cavity offer the possibility to study the kinetics of (bio)chemical processes that involve paramagnetic species. Temperature jumps have been combined with many spectroscopic probing techniques, and EPR would be a useful extension. For a solution of H_2O/glycerol and starting at temperatures below 0 °C, temperature jumps of about 50 °C have been demonstrated. For H_2O, similar temperature jumps were achieved, but higher intensities of IR radiation are necessary.

In conclusion, we have demonstrated two second-moment parameters, $\langle \Delta {B_0}^2 \rangle$ and $\langle \Delta I^2 \rangle$, of a nitroxide EPR spectrum as sensitive reporters of temperature in a broad temperature range. We emphasize that $\langle \Delta I^2 \rangle$ is useful in the fast-motion regime, where other parameters lack sensitivity. The $\langle \Delta I^2 \rangle$ parameter has been used to calibrate temperature jumps of an aqueous sample in the cavity of an EPR spectrometer induced by IR absorption. These experiments set the stage for kinetic studies of processes involving paramagnetic species, in particular for high-frequency EPR spectrometers equipped with single-mode cavities, where submicroliter samples allow homogeneous heating. Such studies are in progress in our laboratory.

■ ASSOCIATED CONTENT

Supporting Information

The Supporting Information is available free of charge on the ACS Publications website at DOI: 10.1021/acs.jpcb.5b08353.

Figures S1−S7 (PDF)

■ AUTHOR INFORMATION

Corresponding Author

*Tel +31(0)71 527 5914; Fax +31(0)71 527 5936; e-mail groenen@physics.leidenuniv.nl (E.J.J.G.).

Notes

The authors declare no competing financial interest.

■ ACKNOWLEDGMENTS

The research was supported with financial aid by The Netherlands Organization for Scientific Research (NWO), Department of Chemical Sciences (CW).

■ REFERENCES

(1) Berliner, L. J.; Reuben, J. *Spin-labeling. Theory and Applications*; Plenum Publishing Corp.: New York, 1989.

(2) Schneider, D. J.; Freed, J. H. In *Spin-labeling. Theory and Applications*; Berliner, L. J., Reuben, J., Eds.; Plenum Publishing Corp.: New York, 1989; pp 1−76.

(3) Redfield, A. G. The Theory of Relaxation Processes. *Adv. Magn. Opt. Reson.* **1965**, *1*, 1−32.

(4) Kirilina, E. P.; Prisner, T. F.; Bennati, M.; Endeward, B.; Dzuba, S. A.; Fuchs, M. R.; Möbius, K.; Schnegg, A. Molecular Dynamics of Nitroxides in Glasses as Studied by Multi-Frequency EPR. *Magn. Reson. Chem.* **2005**, *43*, S119−S129.

(5) Eckburg, J. J.; Chato, J. C.; Liu, K. J.; Grinstaff, M. W.; Swartz, H. M.; Suslick, K. S.; Auteri, F. P. The Measurement of Temperature with Electron Paramagnetic Resonance Spectroscopy. *J. Biomech. Eng.* **1996**, *118*, 193−200.

(6) Alonso, A.; Gonçalves dos Santos, J.; Tabak, M. Stratum Corneum Protein Mobility as Evaluated by a Spin Label Maleimide Derivative. *Biochim. Biophys. Acta, Protein Struct. Mol. Enzymol.* **2000**, *1478*, 89−101.

(7) Dreher, M. R.; Ichikawa, K.; Barth, E. D.; Chilkoti, A.; Rosen, G. M.; Halpern, H. J.; Dewhirst, M. Nitroxide Conjugate of a Thermally Responsive Elastin-Like Polypeptide for Noninvasive Thermometry. *Med. Phys.* **2004**, *31* (10), 2755−2762.

(8) Earle, K. A.; Budil, D. E.; Freed, J. H. 250-GHz EPR of Nitroxides in the Slow-Motional Regime: Models of Rotational Diffusion. *J. Phys. Chem.* **1993**, *97*, 13289−13297.

(9) Earle, K. A.; Moscicki, J. K.; Polimeno, A.; Freed, J. H. A 250 GHz ESR Study of o-Terphenyl: Dynamic Cage Effects above T_c. *J. Chem. Phys.* **1997**, *106* (24), 9996−10015.

(10) Kubelka, J. Time-Resolved Methods in Biophysics. 9. Laser Temperature-Jump Methods for Investigating Biomolecular Dynamics. *Photochem. Photobiol. Sci.* **2009**, *8*, 499−512.

(11) Callender, R.; Dyer, R. B. Probing Protein Dynamics Using Temperatrue Jump Relaxation Spectroscopy. *Curr. Opin. Struct. Biol.* **2002**, *12* (5), 628−633.

(12) Gruebele, M.; Sabelko, J.; Ballew, R.; Ervin, J. Laser Temperature Jump Induced Protein Refolding. *Acc. Chem. Res.* **1998**, *31*, 699−707.

(13) Eaton, W. A.; Muñoz, V.; Hagen, S. J.; Jas, G. S.; Lapidus, L. J.; Henry, E. R.; Hofrichter, J. Fast Kinetics and Mechanisms in Protein Folding. *Annu. Rev. Biophys. Biomol. Struct.* **2000**, *29*, 327−359.

(14) Czerlinski, G.; Eigen, M. Eine Temperatursprungmethode zur Untersuchung Chemischer Relaxation. *Z. Elektrochem., Ber. Bunsenges. Phys. Chem.* **1959**, *63*, 652−661.

(15) Staerk, H.; Czerlinski, G. Nanosecond Heating of Aqueous Systems by Giant Laser Pulses. *Nature* **1965**, *205*, 63−64.

(16) Turner, D. H.; Flynn, G. W.; Sutin, N.; Beitz, J. V. Laser Raman Temperature-Jump Study of the Kinetics of the Triiodide Equilibrium. Relaxation Times in the 10^{-8}−10^{-7} Second Range. *J. Am. Chem. Soc.* **1972**, *94*, 1554−1559.

(17) Gilmanshin, R.; Williams, S.; Callender, R. H.; Woodruff, W. H.; Dyer, R. B. Fast Events in Protein Folding: Relaxation Dynamics of Secondary and Tertiary Structure in Native Apomyoglobin. *Proc. Natl. Acad. Sci. U. S. A.* **1997**, *94*, 3709−3713.

(18) Phillips, C. M.; Mizutani, Y.; Hochstrasser, R. M. Ultrafast Thermally-Induced Unfolding of RNAse-A. *Proc. Natl. Acad. Sci. U. S. A.* **1995**, *92*, 7292−7296.

(19) Decatur, S. M. Elucidation of Residue-Level Structure and Dynamics of Polypeptides via Isotope-Edited Infrared Spectroscopy. *Acc. Chem. Res.* **2006**, *39*, 169−175.

(20) Takahashi, S.; Yeh, S.; Das, T. K.; Chan, C.; Gottfried, D. S.; Rousseau, D. L. Folding of Cytochrome c Iniciated by Submillisecond Mixing. *Nat. Struct. Biol.* **1997**, *4*, 44−50.

(21) Mines, G. A.; Pascher, T.; Lee, S. C.; Winkler, J. R.; Gray, H. B. Cytochrome c Folding Triggered by Electron Transfer. *Chem. Biol.* **1996**, *3*, 491−497.

(22) Nölting, B.; Golbik, R.; Fersht, A. R. Submillisecond Events in Protein-Folding. *Proc. Natl. Acad. Sci. U. S. A.* **1995**, *92*, 10668−10672.

(23) Chan, C.; Hu, Y.; Takahashi, S.; Rousseau, D. L.; Eaton, W. A.; Hofrichter, J. Submillisecond Protein Folding Kinetics Studied by Ultrarapid Mixing. *Proc. Natl. Acad. Sci. U. S. A.* **1997**, *94*, 1779−1784.

(24) Sadqi, M.; Lapidus, L. J.; Muñoz, V. How Fast Is Protein Hydrophobic Collapse? *Proc. Natl. Acad. Sci. U. S. A.* **2003**, *100*, 12117−12122.

(25) Bayley, P.; Martin, S.; Anson, M. Temperature-Jump Circular-Dichroism − Observation of Chiroptical Relaxation Processes at Millisecond Time Resolution. *Biochem. Biophys. Res. Commun.* **1975**, *66*, 303−308.

(26) Chen, E.; Wen, Y.; Lewis, J. W.; Goldbeck, R. A.; Kliger, D. S.; Strauss, C. E. M. Nanosecond Laser Temperature-Jump Optical Rotatory Dispersion: Application to Early Events in Protein Folding/Unfolding. *Rev. Sci. Instrum.* **2005**, *76*, 083120.

(27) Blok, H.; Disselhorst, J. A. J. M.; van der Meer, H.; Orlinskii, S. B.; Schmidt, J. A Continuous-Wave and Pulsed Electron Spin Resonance Spectrometer Operating at 275 GHz. *J. Magn. Reson.* **2005**, *173*, 49−53.
(28) Stoll, S.; Schweiger, A. EasySpin, a Comprehensive Software Package for Spectral Simulation and Analysis in EPR. *J. Magn. Reson.* **2006**, *178* (1), 42−55.
(29) Snipes, W.; Cupp, J.; Cohn, G.; Keith, A. Electron Spin Resonance Analysis of the Nitroxide Spin Label 2.2.6.6-Tetramethyl-piperidone-N-oxyl (Tempone) in Single Crystals of the Reduced Tempone Matrix. *Biophys. J.* **1974**, *14*, 20−32.
(30) Segur, J. B.; Oberstar, H. E. Viscosity of Glycerol and Its Aqueous Solutions. *Ind. Eng. Chem.* **1951**, *43* (9), 2117−2120.
(31) Hubbell, W. L.; Altenbach, C. Investigation of Structure and Dynamics in Membrane Proteins Using Site-Directed Spin Labeling. *Curr. Opin. Struct. Biol.* **1994**, *4*, 566−573.
(32) Marsh, D. EPR Moments for Site-directed Spin-labelling. *J. Magn. Reson.* **2014**, *248*, 66−70.

DOI: 10.1021/acs.jpcb.5b08353
J. Phys. Chem. B 2015, 119, 13416−13421